Biomaterials 32 (2011) 5515–5523

Contents lists available at ScienceDirect

Biomaterials

journal homepage: www.elsevier.com/locate/biomaterials

Genomic instability of gold nanoparticle treated human lung fibroblast cells

Jasmine J. Li [a,d], Soo-Ling Lo [a], Cheng-Teng Ng [a,d], Resham Lal Gurung [b], Deny Hartono [d], Manoor Prakash Hande [b], Choon-Nam Ong [c], Boon-Huat Bay [a,*], Lin-Yue Lanry Yung [d,*]

[a] Department of Anatomy, Yong Loo Lin School of Medicine, National University of Singapore, Singapore 119260, Singapore
[b] Department of Physiology, Yong Loo Lin School of Medicine, National University of Singapore, Singapore 119260, Singapore
[c] Department of Epidemiology and Public Health, Yong Loo Lin School of Medicine, National University of Singapore, Singapore 119260, Singapore
[d] Department of Chemical & Biomolecular Engineering, Faculty of Engineering, National University of Singapore, Singapore 119260, Singapore

ARTICLE INFO

Article history:
Received 16 February 2011
Accepted 6 April 2011
Available online 2 May 2011

Keywords:
Gold nanoparticles
Proteomic analysis
Lung fibroblast
Genotoxicity

ABSTRACT

Gold nanoparticles (AuNPs) are one of the most versatile and widely researched materials for novel biomedical applications. However, the current knowledge in their toxicological profile is still incomplete and many on-going investigations aim to understand the potential adverse effects in human body. Here, we employed two dimensional gel electrophoresis to perform a comparative proteomic analysis of AuNP treated MRC-5 lung fibroblast cells. In our findings, we identified 16 proteins that were differentially expressed in MRC-5 lung fibroblasts following exposure to AuNPs. Their expression levels were also verified by western blotting and real time RT-PCR analysis. Of interest was the difference in the oxidative stress related proteins (NADH ubiquinone oxidoreductase (NDUFS1), protein disulfide isomerase associate 3 (PDIA3), heterogeneous nuclear ribonucleus protein C1/C2 (hnRNP C1/C2) and thioredoxin-like protein 1 (TXNL1)) as well as proteins associated with cell cycle regulation, cytoskeleton and DNA repair (heterogeneous nuclear ribonucleus protein C1/C2 (hnRNP C1/C2) and Secernin-1 (SCN1)). This finding is consistent with the genotoxicity observed in the AuNP treated lung fibroblasts. These results suggest that AuNP treatment can induce oxidative stress-mediated genomic instability.

1. Introduction

The current knowledge of the toxicological profile of gold nanoparticles (AuNPs) is incomplete and this is inhibiting their use in many clinical applications including diagnostic imaging [1], drug delivery [2,3] and photothermal therapy [4]. Bulk gold is a yellow solid and relatively inert, while AuNPs at nanosize appear wine red in solution and their biological activity is still not entirely understood. The unique characteristics and properties of the nanosized particles also make it hard to predict their biological reactivity. Some studies have suggested that AuNPs may cause toxicity *in vitro*, citing oxidative stress and DNA damage as results of AuNP treatment [5,6,7]. *In vivo* studies also reflect similar observations; AuNPs exhibited pulmonary toxicity and genotoxicity in mice as well as oxidative stress in aquatic species [8,9]. One study on inhalation exposed rats to AuNPs also showed differential expression in global gene analysis in various organ tissues [10]. As we had previously reported, AuNP treatment also induces oxidative stress, autophagy and DNA damage *in vitro* [5,11]. It would seem that, there is still a need to perform in depth investigations on the toxicity profile of AuNPs for its use in bio-applications to be safe and meaningful.

Proteomic techniques, such as two dimensional gel electrophoresis (2D-GE), are useful tools in the field of drug and toxicity studies. In 2D-GE, proteins are separated according to 2 measures, firstly by their isoelectric points and secondly by molecular weight through SDS-PAGE gel electrophoresis. It is one of the most common tools currently used in toxicity studies today. Coupling it with mass spectrometry, specifically the matrix-assisted laser desorption/ionization time-of-flight mass spectrometry (MALDI TOF MS), allows the identification of protein biomarkers of disease progression or predictive markers of toxicogenesis [12]. The use of proteomic techniques in toxicological studies is steadily growing as the field relies more heavily on molecular data to identify critical protein changes and pathways to provide a reliable predictive platform for drug development and toxicological profiling [13,14]. A number of

* Corresponding authors. Tel.: +65 6516 1699.
E-mail addresses: antbaybh@nus.edu.sg (B.-H. Bay), cheyly@nus.edu.sg (L.-Y.L. Yung).

0142-9612/$ – see front matter © 2011 Elsevier Ltd. All rights reserved.
doi:10.1016/j.biomaterials.2011.04.023

researches have classified the use of proteomics in toxicity studies into two levels. Tier I analysis refers to global protein mapping and profiling for differential expression while Tier II involves elucidating the protein functions and interactions as well as how specific post-translational modifications and their threedimensional structure affect these processes [14].

The primary focus of the current study was on the quantification and identification of proteins (Tier I analysis) and its differential expression upon AuNP treatment since nanomaterial-induced toxicological profiles are still largely unknown. We performed a comparative analysis of the protein expression profile of AuNP treated and control human fetal MRC-5 lung fibroblasts. To confirm the proteomic findings, selected protein expression results were verified by western blotting and real time RT-PCR analysis. In addition, we further correlated the above investigations with the alkaline single-cell gel electrophoresis assay (comet assay) and the fluorescence *in situ* hybridization (FISH) assay to assess DNA damage and chromosomal aberrations caused by *in vitro* exposure to AuNPs.

2. Materials & methods

2.1. Cell culture

The cells used were MRC-5 human fetal lung fibroblast cells (ATCC No.: CCL-171) cultured in RPMI 1640 media and supplemented with 10% fetal bovine serum (FBS) in 100 μg/ml penicillin/streptomycin in a 37 °C, 5% CO_2 incubator.

2.2. AuNP synthesis and preparation

Gold nanoparticles (AuNPs) of 20 nm in diameter, were prepared in citrate reduction from gold salts. The nanoparticles were spun down to remove the citrate buffer and subsequently coated with fetal bovine serum, washed and reconstituted in phosphate buffer saline (PBS) solution to form the stock solution. The AuNP stock solution was then sterile filtered before addition into treatment media.

2.3. AuNP treatment

MRC-5 cells were seeded in 6 wells cell culture plates (NUNC) at a seeding density of 4×10^4 cells/ml and treated with 1 nM concentration of AuNP in growth media the following day. Control cells were cultured in growth media. Treated and control cells were then incubated for 72 h before harvesting.

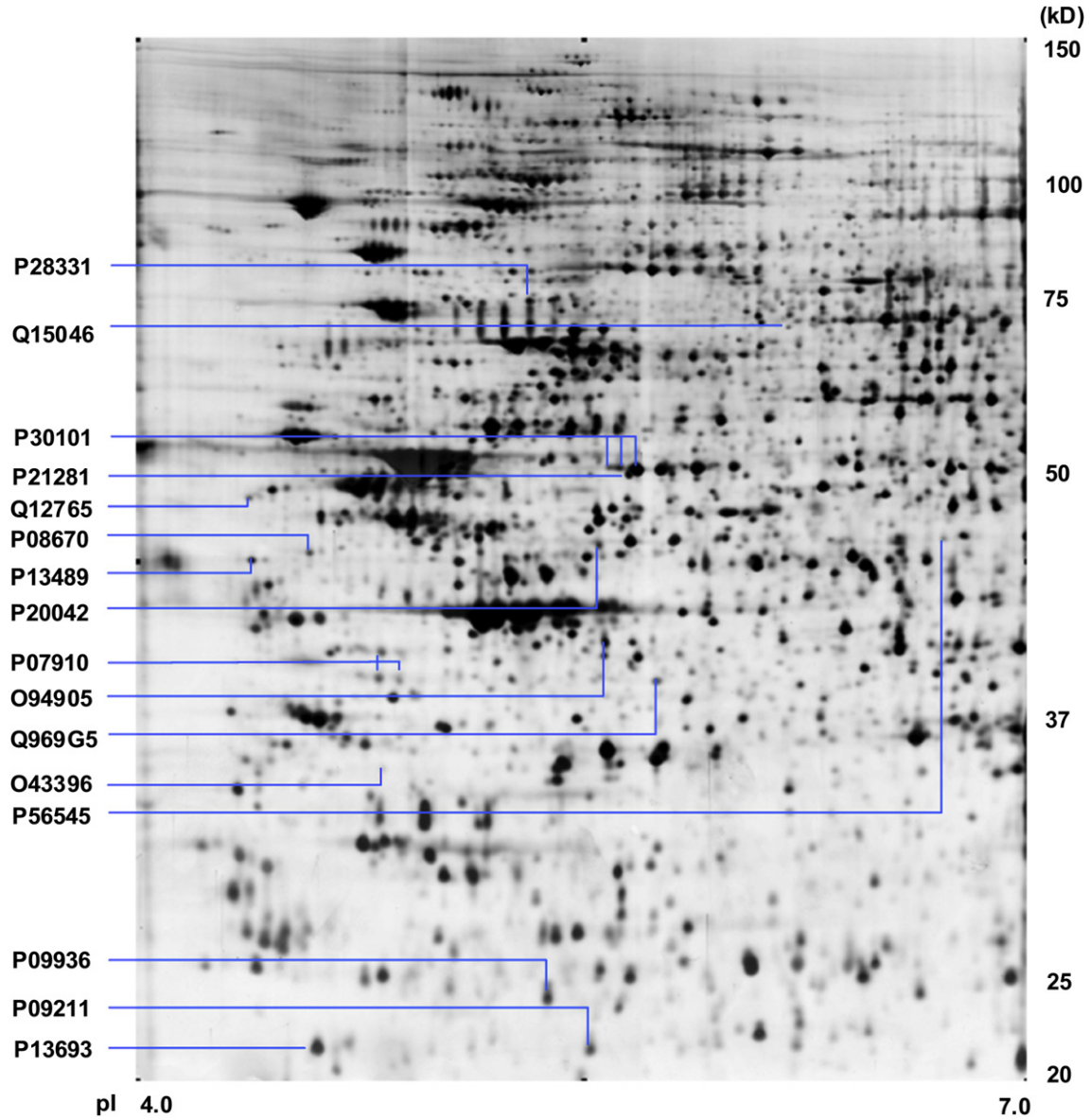

Fig. 1. Representative map of silver-stained two dimensional electrophoresis from MRC-5 whole cell lysate focused on a non-linear pH 4–7 IPG strip. Sixteen proteins identified were labeled with their respective Swiss-Prot accession numbers.

Table 1
List of protein spots undergoing quantitative changes with AuNP treatment as identified by MALDI-TOF/TOF MS.

Protein name[a]	Accession no.[a]	Protein score/% coverage[b]	Mr (Da)/PI[b]	Control vs treatment[c,d]	*t*-test (*p*-value)
NADH ubiquinone oxidoreductase	P28331	664/45	80,443/5.89	+12.1171	<0.0001
Lysyl-tRNA synthetase	Q15046	130/11	68,461/5.94	+2.7730	0.0052
Protein disulfide isomerase associated 3	P30101	440/25	54,454/6.78	Not detected in control	NA
		428/36	54,454/6.78	Not detected in control	NA
		926/45	54,454/6.78	+1.4547	0.0461
V-type proton ATPase subunit B	P21281	891/60	55,708/5.40	+3.2155	0.0383
Secernin-1	Q12765	141/13	47,020/4.69	−1.5945	0.0041
Vimentin	P08670	794/66	49,680/5.19	−1.8346	0.0023
Ribonuclease inhibitor	P13489	102/42	51,766/4.71	+1.6793	0.0195
Eukaryotic translation initiation factor 2 subunit 2	P20042	84/15	38,706/5.60	+1.5887	0.0031
Heterogeneous nuclear ribonucleoproteins C1/C2	P07910	430/25	32,375/4.94	−1.7400	0.0006
		54/15	32,375/4.94	−1.8196	0.0007
		55/12	32,375/4.94	−1.6838	0.0061
Erlin 2	O94905	216/51	38,044/5.47	+1.5043	0.0004
Protein kinase C delta-binding protein	Q969G5	429/38	27,685/6.05	−1.5111	0.0013
Thioredoxin-like protein 1	O43396	129/53	32,630/4.84	−2.3040	0.0002
C-terminal-binding protein 2	P56545	125/33	49,427/6.47	−1.5745	0.0024
Ubiquitin carboxyl terminal hydrolase isozyme L1	P09936	287/48	25,151/5.33	+2.3386	0.0085
Glutathione S-transferase P	P09211	406/47	23,569/5.43	+2.8476	0.0026
Translationally-controlled tumor protein	P13693	184/45	19,697/4.84	+2.9485	0.0019

[a] Protein name and accession numbers were derived from Swiss-Prot.
[b] Protein score, percentage of coverage and Mr (Da)/PI were derived from MASCOT.
[c] Protein spots were quantified based on the normalized average percentage of volume derived from ImageMaster 2D Platinum 6.0 software analysis.
[d] Approximate fold-changes of protein expression were derived from the ratio of normalized average percentage of volume of treatment to control protein spots or vice versa. A "+" indicates upregulation in the nano gold particles treated samples while "−" indicates downregulation.

2.4. Protein extraction

Cells were washed once in PBS and then twice in 0.35 M sucrose to minimize contamination with salts. The cells were then harvested with a cell scrapper in 0.35 M sucrose containing proteinase inhibitor mix (Amersham Biosciences). The cell pellets were collected after centrifugation at 2000 rpm for 5 min at 4 °C and was subsequently resuspended in lyses buffer containing 7 M urea, 2 M thiourea, 4% CHAPS, 20 mM dithiothreitol, 0.5% Pharmalyte pH 4–7, proteinase inhibitor mix and nuclease mix (Amersham Biosciences). Protein concentrations were determined using a 2 D Quant Kit (Amersham Biosciences).

2.5. Two dimensional gel electrophoresis (2D-GE)

For analytical and preparative gels, approximately 80 ug and 240 ug respectively, of proteins were loaded into the rehydrated 18 cm non-linear Immobilized pH gradient (IPG) strip (pH 4–7) using the cup-loading method. The first dimensional isoelectric focusing (IEF) run was carried out using the following conditions: (i) 300 V, 450 V h; (ii) 500 V, 250 V h; (iii) 1000 V, 1000 V h; (iv) 1000–8000 V, 3500 V h and (v) 8000 V, 32,000 V h. Voltage increases for (i), (ii), (iii), and (v) were performed on a "stepwise" basis, while the increase for (iv) was on a "linear gradient". This was followed by the second dimensional SDS-PAGE, performed on 1.0 mm 9% polyacrylamide gels at a constant power of 10 W per gel at 16 °C by using Ettan DALTsix electrophoresis system (Amersham Biosciences). All samples were run in triplicate to ensure reproducibility.

2.6. Protein visualization and image analysis

2 D gels were visualized by staining with PlusOne silver staining kit (GE Healthcare) according to manufacturer's instructions. Silver-stained gels were scanned by an image scanner and all the triplicate gels were then analyzed with ImageMaster 2D Platinum 6.0 (GE Healthcare).

2.7. In-gel reduction, alkylation and trypsin digestion of protein spots

Silver-stained protein spots were excised manually and cut into small pieces. The gel pieces were dehydrated in 100 μl of 100% acetonitrile, dried and rehydrated in 20 ul of solution containing 10 mM dithiothreitol in 100 mM ammonium bicarbonate. Further preparation involved repeated wash and dehydration steps with ammonium bicarbonate and acetonitrile. The gel pieces were subsequently digested with 10 μl of 0.01 μg/μl sequencing grade modified trypsin (Promega) in 50 mM ammonium bicarbonate and incubated at 37 °C for 14 h. To enhance peptide extraction, 10 μl of 0.1% trifluoroacetic acid in 50% acetonitrile was added to the gel pieces for final extraction. The extracts were dried in a Speedvac before mass spectrometry analysis.

2.8. MALDI-TOF/TOF MS and protein identification

Dried extract was re-dissolved in 1 μl of matrix solution containing 5 mg/ml of a-cyano-4 hydroxycinnamic acid (CHCA) in 0.1% trifluoroacetic acid and 50% acetonitrile. The extract was spotted onto the MALDI target plate, and allowed to dry in air, prior to mass spectrometry analysis using an Applied Biosystems 4800 Proteomics Analyzer MALDI-TOF/TOF Mass Spectrometer (Framingham). For the purposes of peptide and protein identification, the GPS explorer™ software Version 3.6 (Applied Biosystems) was used to create and search files with the MASCOT search engine (Version 2.1; Matrix Science).

2.9. Western blotting

Protein extracted from cell lysates as described above was resolved on SDS-PAGE gel and transferred onto PVDF membrane via semidry transfer (BioRad). Membranes were blocked in 5% non-fat milk and washed in Tris-buffered saline with 0.1% Tween. Membranes were incubated with primary antibody, followed by the corresponding secondary antibody with 3 washing steps in between. Protein bands were developed with chemiluminescence substrate (Pierce) and visualized on XPress CL blue ray film (Pierce). Optical densities of bands were measured on the GS710 Densitometer and band intensities were analyzed with Quantity One image analysis software (Biorad). Primary antibodies used were as follows: PDIA3 (ab10287, Abcam) and hnRNP C1/C2 (ab10294, Abcam).

2.10. Real time RT-PCR

MRC-5 cells were treated with AuNPs for 48 h prior to RNA extraction with RNeasy Mini kit (Qiagen). Total RNA was then converted to cDNA with the Superscript III First Strand cDNA Synthesis kit (Invitrogen). Subsequently, real time PCR was carried out on an ABI 7900HT system using the FAST format and SYBR green mastermix (Applied Biosystems). Primer sequences for the genes of interest are listed as follows: Protein disulfide isomerase associate 3 (PDIA3/ERp57) AAG CTC AGC AAA GAC CCA AA (forward), CAC TTA ATT CAC GGC CAC (reverse); V-type proton ATPase B2 (VATB) GAG GGG CAG ATC TAT GTG GA (forward), GGC TTC TTC TCC AAC GAC AG (reverse); heterogeneous nuclear ribonucleus protein C1/C2 (hnRNP CI/C2) TGT GGA GGC AAT CTT TTC GA (forward), TGA TAC ACG CTG ACG TTT CG (reverse); housekeeping gene glyceraldehyde-3-phosphate dehydrogenase (GAPDH) GAA GGT GAA GGT CGG AGT CAA CG (forward), TGC CAT GGG TGG AAT CAT ATT GG (reverse). Fold change was calculated with the ΔΔ2CT method.

2.11. Alkaline single-cell gel electrophoresis (comet assay)

Treated cells were harvested and washed twice in PBS before resuspending in phosphate buffer saline solution (PBS). The cells were embedded in 0.8% low melting agarose (Pronadisa, Spain) on comet slides (Trevigen) and lysed in pre-chilled lysis solution (2.5 M NaCl, 0.1 M EDTA, 10 mM Tris base, pH 10) with 1% Triton × (Trevigen) for 1 h at 4 °C. Cells were then subjected to denaturation in

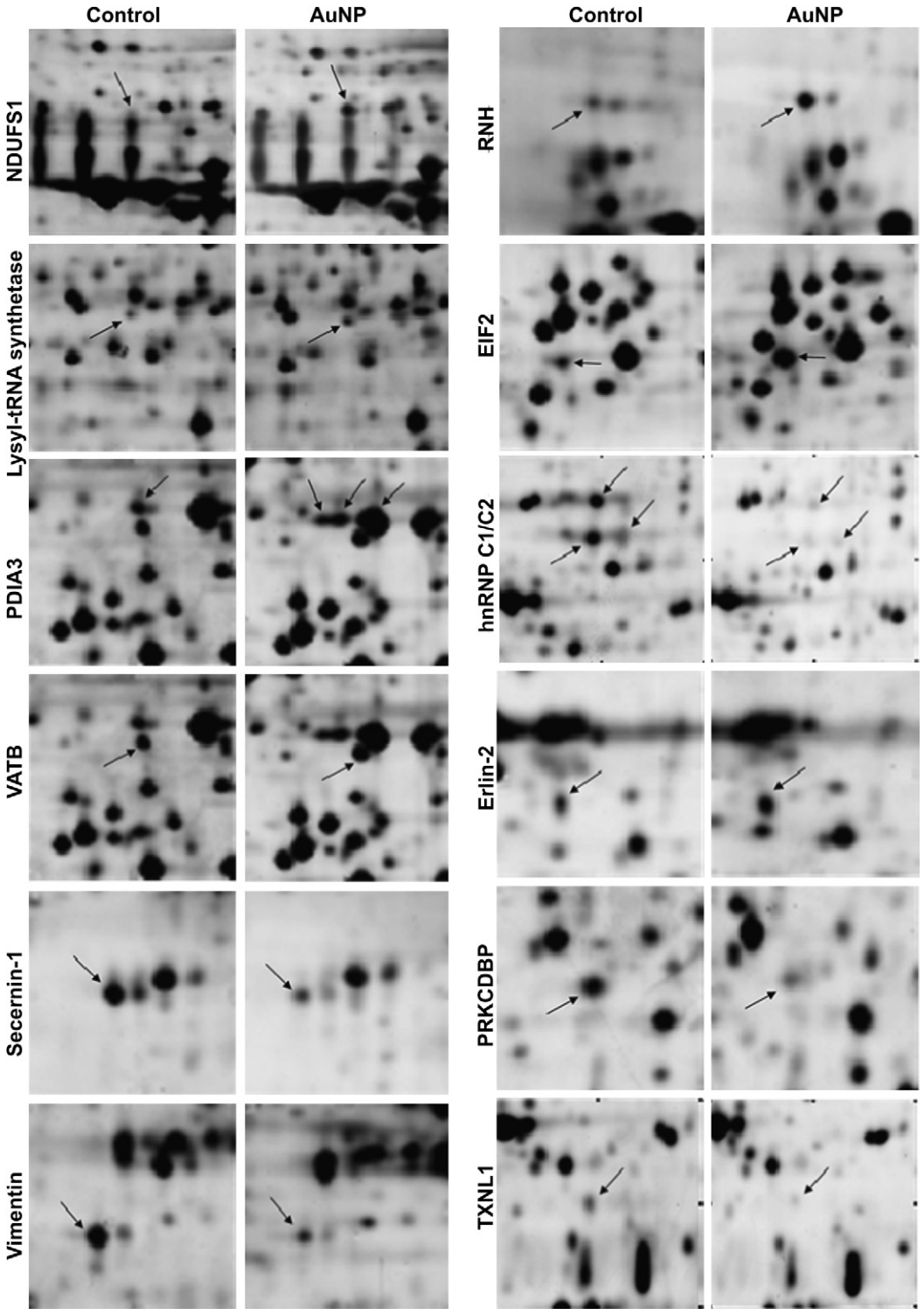

Fig. 2. Two dimensional gel electrophoresis (2D-GE) of AuNPs treated cellular protein extracts. Arrows with respective labels indicate protein spots with significant differences in expression. Comparing control and AuNP treated samples reveal spot differences. Upon mass spectrometry analysis, protein spots were identified as indicated.

alkaline buffer (0.3 M NaCl, 1 mM EDTA) for 40 min in the dark at room temperature. Electrophoresis was performed at 25 V and 300 mA for 20 min. The slides were immersed in neutralization buffer (0.5 M Tris-HCl, pH 7.5) for 15 min followed by dehydration in 70% ethanol. Subsequently they were air-dried and stained with SYBR green dye. The tail moments of the nuclei were measured as a function of DNA damage. Analysis was done using comet imager v1.2 software (Metasystems GmbH). 50 comets were analyzed per concentration. Experiments were done in duplicates.

2.12. Florescence in situ hybridization assay (FISH assay)

The FISH assay detects and identifies types of DNA damage and aberrations. MRC-5 cells were treated in the typical condition of 1 nM AuNP for 72 h and allowed to grow for another 24 h in the absence of AuNPs. The cells were subsequently arrested at mitosis by treatment with colcemid (0.1 μg/ml) in media. Cells were then fixed in Carnoy's fixative and then incubated with a hypotonic solution (0.075 M KCl) at 37 C for 15 min. Subsequently, cells were stained with telomere specific peptide

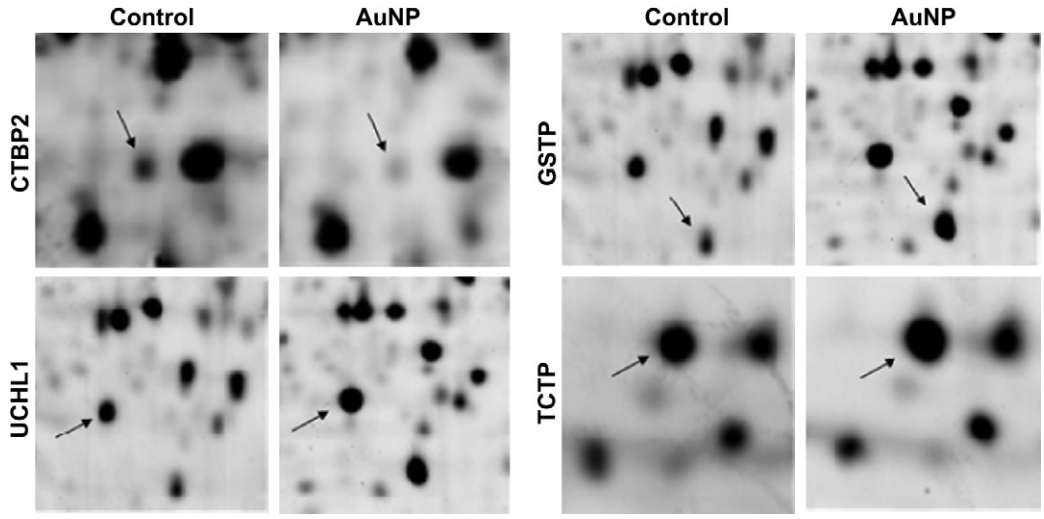

Fig. 2. (*continued*).

nucleic acid (PNA) probes labeled with Cyc3 and centromere specific PNA probes labeled with FITC. The cells were counterstained with 4′,6-diamidino-2-phenylindole (DAPI) to visualize the chromosomes. Metaphase spreads (50 per treatment) were captured on a Zeiss Axioplan 2 imaging fluorescence microscope (Carl Zeiss) and analysed using the *in situ* imaging software (Metasystems GmbH).

2.13. Statistical analysis

All statistical analyses were performed on the Graphpad Prism 4.0 software. Statistical analyses of the values for all experiments are expressed as mean ± standard deviation. The data were analyzed using *Student's t test* or One-Way ANOVA (Graphpad Prism, USA). Those with $p < 0.05$ are considered as significant.

3. Results

3.1. Two dimensional gel electrophoresis

Sixteen proteins were found to be differentially expressed in the treated samples (Fig. 1, Table 1, $p < 0.05$). The identities of these proteins were revealed by mass spectrometry as shown in Fig. 2. Of particular interests are many of the proteins associated with the oxidative stress pathways. There was a 12 fold upregulation of NADH ubiquinone oxidoreductase (NDUFS1) and a 2.7 fold upregulation for disulfide isomerase associated 3 (PDIA3) protein (also known as ER60 or ERp57), an endoplasmic reticulum protein associated with cellular stress [15] (Fig. 2 & Table 1; $p < 0.05$). The heterogeneous nuclear ribonucleoproteins C1/2 (hnRNP C1/2), an mRNA binding protein involved in mRNA export, localization, translation and stability [16] showed significant downregulation by almost 2 fold with AuNP treatment as compared to control (Table 1, $p < 0.01$). Thioredoxin-like protein isoform 1 (TXNL1), a thioredoxin which is involved in regulating oxidative stress [17] was observed to be down-regulated by more than 2 fold in the treated samples (Table 1, $p = 0.0002$). Western blotting also confirmed significant downregulation of hnRNP C1/2 expression (Fig. 3, $p < 0.01$) and increased PDIA3 protein expression in AuNP treated samples (Fig. 3, $p < 0.01$). In addition, several proteins associated with cell cycle regulation, cytoskeleton and DNA repair were also affected (Table 1). They include heterogeneous nuclear ribonucleus protein C1/C2 (hnRNP C1/C2) and Secernin-1 (SCN1).

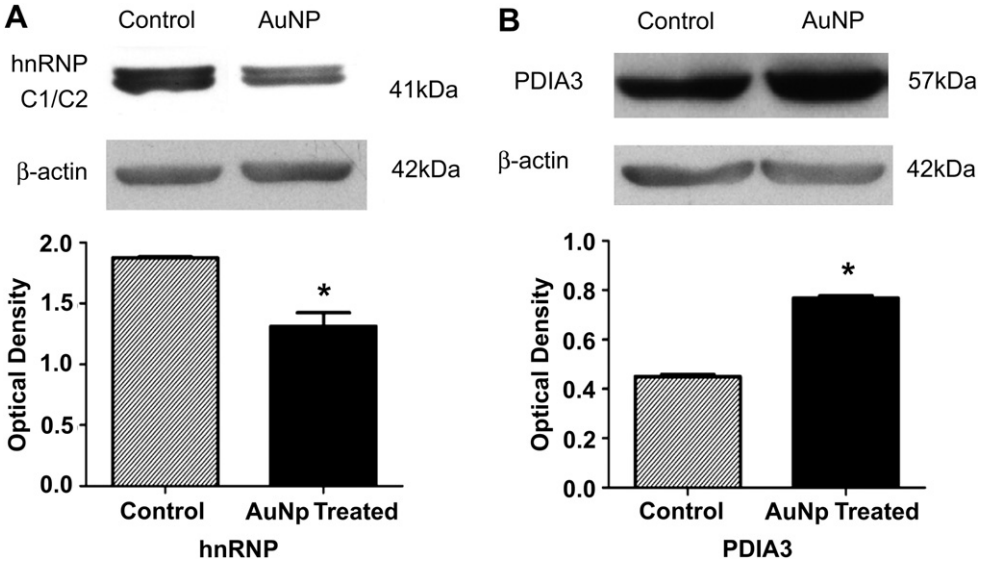

Fig. 3. Western blotting of oxidative stress related proteins hnRNP and PDIA3 proteins. (A) hnRNP antibodies probe for both C1 and C2 isoforms visualised as 2 bands at band size 41 kDa and 43 kDa. Optical density of band intensity of control compared with AuNP treated samples show downregulation of hnRNP protein expression (p-value < 0.01). (B) Conversely, probing with PDIA3 antibodies reveal an upregulation in AuNP treated samples. Optical density of band intensity is significantly higher in AuNP treatment compared to control (p-value < 0.01). Error bars = SEM.

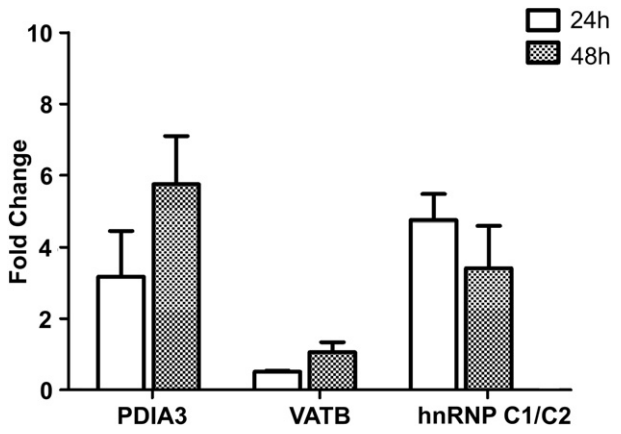

Fig. 4. Fold change of PDIA3, VATB and hnRNP C1/C2 genes from real time RT-PCR analysis at 24 h and 48 h post AuNP treatment. Although results were not significant, the trend in gene expression corresponds with our results in the proteomics assay. PDIA3 and VATB gene expressions showed an upregulation in fold change with time while hnRNP C1/C2 gene expression exhibited a downward trend that matched the decrease in the protein expression level.

3.2. Real time RT-PCR

We further validated our proteomic results with real time RT-PCR for a few selected genes. Although the results were not significant, we detected a trend in the gene expression of PDIA3, VATB and hnRNP C1/C2 over time, which corresponded with the upregulation and downregulations in our proteomic results (Fig. 4).

3.3. Genomic instability assays

The comet assays showed positive results for DNA damage in the AuNP treated MRC-5 lung fibroblasts. Comet tail moments were found to be significantly higher in the treated group than in the control (Fig. 5C, $p < 0.05$). As shown by FISH, AuNP treated cells had a significant > 4 fold increase in aberrations per cell as compared to the controls (Fig. 6A, $p < 0.0001$). All aberrations observed were chromosomal breaks with the majority being undetectable telomeres (Fig. 6C). No chromosomal fusions were found. It would appear that that short-term AuNP treatment is likely to cause chromosomal breaks in MRC-5 fibroblasts that persist even after one population doubling.

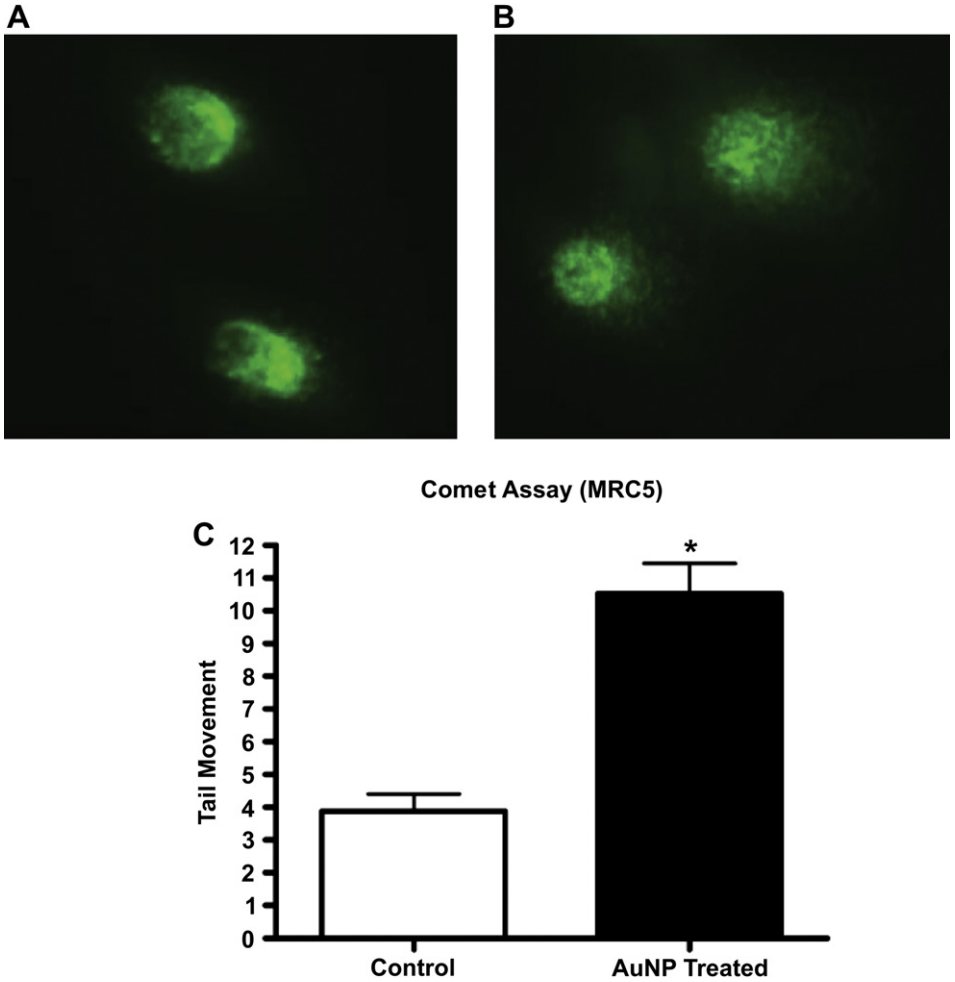

Fig. 5. Comet assay on control and AuNP treated MRC-5 lung fibroblasts. Cells were treated for 72 h in 1 nM AuNP and subsequently run on alkaline electrophoresis and stained in SYBR green which visualizes the comet "tail", the length of which is an indicator of DNA damage. (A) Control cells show little to no tail. (B) AuNP treated cells display a comparatively longer tail, indicative of the presence of higher DNA damage, particularly strand breaks. (C) Analysis of 100 cells per treatment captured by the software showed that AuNP treated cells have significantly higher DNA damage than control (p-value < 0.05). Tail moment is used as the comparative value. Error bars = SEM (For interpretation of the references to colour in this figure legend, the reader is referred to the web version of this article).

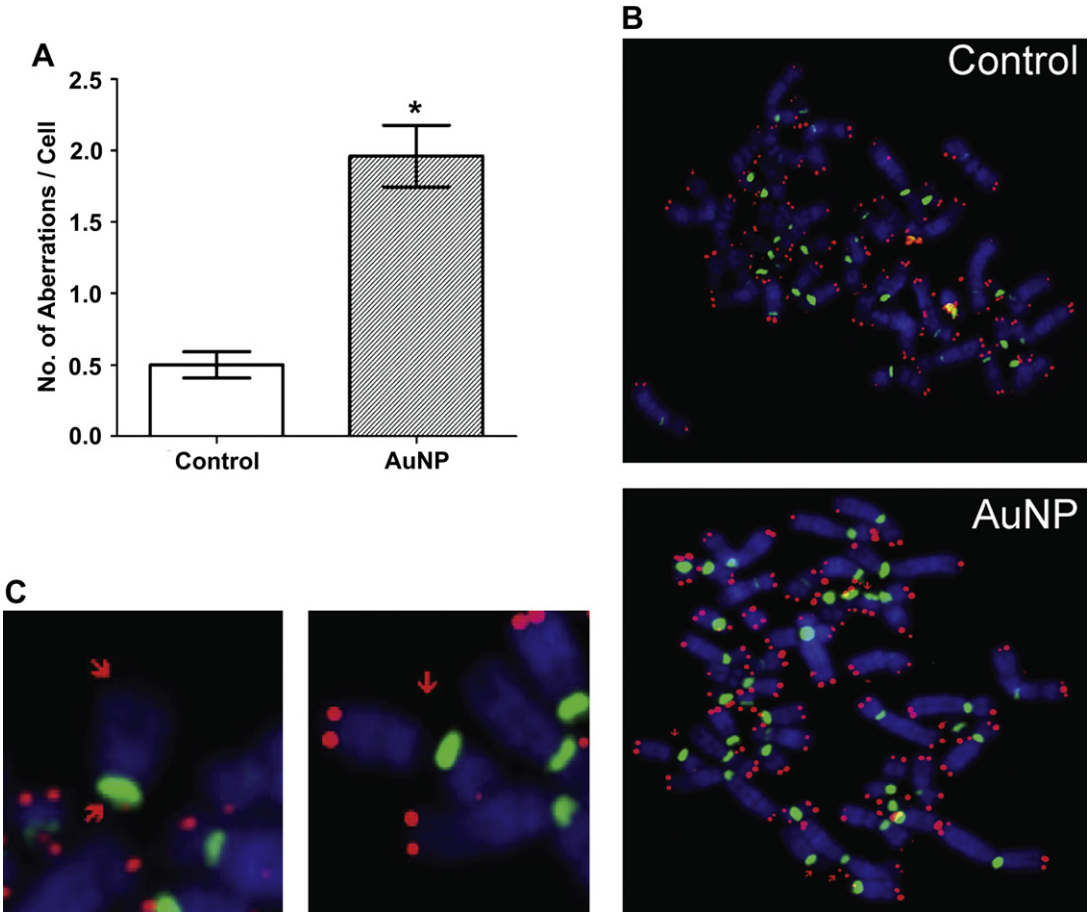

Fig. 6. Fluorescence In Situ Hybridization (FISH) analysis of control and AuNP treated MRC-5 lung fibroblasts (1 nM concentration and 72 h). 50 cells per treatment were analyzed and found to have a higher incidence of chromosomal aberrations in the AuNP treated cells as compared with the untreated controls. Red arrows point to chromosomal aberrations. (A) Bar chart of average number of aberrations per cell ($n = 50$). There is a significant > 4 fold difference between control and treated cells (p-value < 0.0001). Error bars = SEM. (B) Metaphase spreads of control and AuNP treated cells respectively. (C) Chromosomal breaks and undetectable telomere were the aberrations detected. No fusion was observed (For interpretation of the references to colour in this figure legend, the reader is referred to the web version of this articl).

4. Discussion

The 2D-GE technique is a useful tool for global proteomic analysis in toxicity research, and they play an increasingly important role in toxicity biomarker discovery and validation [18,19]. Studies which employ this proteomic technique have been used in experiments involving silica nanoparticles [20], multi-walled carbon nanotubes [21], titanium dioxide nanoparticles [22], airborne particulate matter [23] and silver nanoparticles [24] but there are few on AuNPs [25].

In this present study, the protein NDUFS1 is the core and largest subunit of the mitochondrial membrane respiratory chain NADH dehydrogenase (also known as complex I) was found to be highly upregulated in AuNP treated lung fibroblasts. NDUFS1 is the most basic unit required for catalysis reactions. Complex I functions in the transfer of electrons from NADH to the respiratory chain with ubiquinone as the immediate electron acceptor. It has an iron-sulfur protein (IP) component that forms part of the active site crevice where NADH is oxidized. Hence, complex 1 is known to be the major source of superoxide O_2 and ROS in human fibroblasts [26] which correlates with our previous findings of induction of oxidative stress in AuNP treated cells [5].

AuNP treatment also affects other oxidative stress related proteins, particularly the antioxidant proteins. PDIA3, better known as ER60 or ERp57, is known to display protective ability against H_2O_2 toxicity (oxidative stress) and upon binding to protein Ref-1, are involved in activation of a number of transcription factors [27]. Not surprisingly, the upregulation of this protein is also accompanied by a similar upregulation of various transcription and translation factors in the 2D-GE results. This same complex has also been implicated in DNA repair, as cellular sensors for DNA damage mismatch repairs [28,29]. Increased expression of PDIA3, which has an antioxidant function, is also an appropriate cellular response to oxidative stress and DNA damage caused by AuNP treatment. TXNL1, which is reported to be protective against glucose deprivation cytotoxicity [17] was also down-regulated. Both PDIA3 and TXNL1 are part of the thioredoxin superfamily of which is also known to regulate cellular redox potential and prostaglandin synthase [30].

The downregulation of heterogeneous nuclear ribonucleus protein C1/C2 (hnRNP C1/C2) expression is another point of interest. The main function of this protein is binding to pre-mRNA and nucleates the assembly of 40S hnRNP particles [31]. They also modulate the stability and the level of translation of bound mRNA molecules. Interestingly, downregulation of hnRNP C1/C2 sensitizes cells to stress [32]. Moreover, a number of studies have linked hnRNP C1/C2 with repair of DNA strand breaks [33,34], implicating its role in coordinating DNA repair mechanisms in the cell. Our findings are believed to point towards the non-homologous end-joining (NHEJ) pathway of DNA damage repair in the AuNP treated lung fibroblasts. The comet and the FISH assays in this current study also showed evidence of DNA and chromosomal breaks. Therefore, it is plausible that AuNPs can induce DNA damage and impair DNA repair

responses through the dysregulation of DNA repair genes involved in the NHEJ pathway [11] leading to persistent DNA damage. In our previous paper [5], we found upregulation of polynucleotide kinase (PNK) gene, another gene known to be involved with the NHEJ pathway [35,36] corroborating the results of this present study.

The rest of the differentially expressed proteins are mainly involved as cell cycle regulators or have involvement in the cell cytoskeleton or even possibly tumorigenesis. Vimentins are intermediary filaments found abundantly in fibroblast cells [37]. Secernin-1 (SCN1) is a cytosolic protein with roles in the regulation of exocytosis in mast cells and recently found to be a prognostic marker for gastric cancer [38,39]. Translationally-controlled tumor protein (TCPT) stablizes microtubules and has calcium binding properties [40]. Early translation factor proteins are the eukaryotic translation initiation factor 2 (eIF2-beta) [41] and lysyl-tRNA sythase (lysRNA), the latter also has roles as a proinflammatory signaling molecule and can cause cell toxicity when bound to mutant form of superoxide dismutase [42,43]. The upregulation of these proteins in our study signals the role of these proteins in AuNP-induced oxidative stress in fibroblasts. Another cell cycle protein includes the C-terminal-binding protein II (CtBP2) is known as a corepressor of transcription [44] with important regulatory roles in development and oncogenesis [45]. V-type proton ATPase subunit B2 (VATB2) is part of a larger complex of V-ATPases proton pumps that acidify endocytic and exocytic organelles [46]. Erlin 2 (SPFH2) belongs to a family of prohibitin proteins on the endoplasmic reticulum that degrade IP3 receptions on the ER membrane [47], dysregulation of this protein could disrupt cellular signaling pathways. Glutathione S transferase P (GSTP1-1) is a detoxification enzyme that catalyzes the conjunction of various hydrophilic compounds and electrophilic compounds with glutathione [48]. Ribonuclease inhibitor (RNH) in tissues has strong affinity binding to ribonucleases and recent studies show that it may have anti-tumor effects in hematopoietic cells [49]. Not much is known about protein kinase C delta-binding protein (hSRBC) however it may possess some tumor suppressor properties in primary lung cancers [50]. The ubiquitin carboxyl terminal hydrolase isozyme L1 (UCH-L1) is a thiol protease that has been reported to possess tumor suppressor characteristics in nasopharyngeal carcinomas [51].

5. Conclusion

We have employed the use of 2D-GE proteomic technique to uncover more of the cellular changes occurring within the MRC-5 fibroblasts during AuNP treatment. Proteins that were differentially expressed were found to cover a range of functions including oxidative stress response as well as regulation of cell cycle and cytoskeleton. AuNP treatment also caused sustained DNA strand breaks and chromosomal breaks induced by oxidative stress. We propose that these changes reflect the state of oxidative stress inside the cell and they are cellular responses of protection and repair.

Acknowledgement

This work was supported by research funding from the Singapore Ministry of Education Academic Research Fund Tier 2 via grant MOE2008-T2-1-046.

References

[1] van Schooneveld MM, Cormode DP, Koole R, van Wijngaarden JT, Calcagno C, Skajaa T, et al. A fluorescent, paramagnetic and PEGylated gold/silica nanoparticle for MRI, CT and fluorescence imaging. Contrast Media Mol Imaging 2010;5(4):231–6.
[2] Paciotti GF, Myer L, Weinreich D, Goia D, Pavel N, McLaughlin RE, et al. Colloidal gold: a novel nanoparticle vector for tumor directed drug delivery. Drug Deliv 2004;11(3):169–83.
[3] Kim CK, Ghosh P, Rotello VM. Multimodal drug delivery using gold nanoparticles. Nanoscale 2009;1(1):61–7.
[4] Wang S, Chen KJ, Wu TH, Wang H, Lin WY, Ohashi M, et al. Photothermal effects of supramolecularly assembled gold nanoparticles for the targeted treatment of cancer cells. Angew Chem Int Ed Engl 2010;49(22):3777–81.
[5] Li JJ, Hartono D, Ong CN, Bay BH, Yung LYL. Autophagy and oxidative stress associated with gold nanoparticles. Biomaterials 2010;31(23):5996–6003.
[6] Pan Y, Leifert A, Ruau D, Neuss S, Bornemann J, Schmid G, et al. Gold nanoparticles of diameter 1.4 nm trigger necrosis by oxidative stress and mitochondrial damage. Small 2009;5(18):2067–76.
[7] Jia HY, Liu Y, Zhang XJ, Han L, Du LB, Tian Q, et al. Potential oxidative stress of gold nanoparticles by induced-NO releasing in serum. J Am Chem Soc 2009;131(1):40–1.
[8] Jacobsen NR, Moller P, Jensen KA, Vogel U, Ladefoged O, Loft S, et al. Lung inflammation and genotoxicity following pulmonary exposure to nanoparticles in ApoE-/- mice. Part Fiber Toxicol 2009;6:2.
[9] Tedesco S, Doyle H, Redmond G, Sheehan D. Gold nanoparticles and oxidative stress in Mytilus edulis. Mar Environ Res 2008;66(1):131–3.
[10] Yu LE, Yung LYL, Ong CN, Tan YL, Balasubramaniam KS, Hartono D, et al. Translocation and effects of gold nanoparticles after inhalation exposure in rats. Nanotoxicology 2007;1(3):235–42.
[11] Li JJ, Zou L, Hartono D, Ong CN, Bay BH, Yung LYL. Gold nanoparticles induce oxidative damage in lung fibroblasts in vitro. Adv Mater 2008;20(1):138–42.
[12] George J, Singh R, Mahmood Z, Shukla Y. Toxicoproteomics: new paradigms in toxicology research. Toxicol Mech Methods 2010;20(7):415–23.
[13] Bandara LR, Kennedy S. Toxicoproteomics – a new preclinical tool. Drug Discov Today 2002;7(7):411–8.
[14] Merrick BA, Witzmann FA. The role of toxicoproteomics in assessing organ specific toxicity. EXS 2009;99:367–400.
[15] Frickel E-M, Frei P, Bouvier M, Stafford WF, Helenius A, Glockshuber R, et al. ERp57 is a multifunctional thiol-disulfide oxidoreductase. J Biol Chem 2004;279(18):18277–87.
[16] Dreyfuss G, Kim VN, Kataoka N. Messenger-RNA-binding proteins and the messages they carry. Nat Rev Mol Cell Biol 2002;3(3):195–205.
[17] JimÈnez A, Pelto-Huikko M, Gustafsson J-A, Miranda-Vizuete A. Characterization of human thioredoxin-like-1: potential involvement in the cellular response against glucose deprivation. FEBS Lett 2006;580(3):960–7.
[18] Johnson CJ, Zhukovsky N, Cass AE, Nagy JM. Proteomics, nanotechnology and molecular diagnostics. Proteomics 2008;8(4):715–30.
[19] Sheehan D. The potential of proteomics for providing new insights into environmental impacts on human health. Rev Environ Health 2007;22(3):175–94.
[20] Yang X, Liu J, He H, Zhou L, Gong C, Wang X, et al. SiO_2 nanoparticles induce cytotoxicity and protein expression alteration in HaCaT cells. Part Fiber Toxicol 2010;7:1.
[21] Witzmann FA, Monteiro-Riviere NA. Multi-walled carbon nanotube exposure alters protein expression in human keratinocytes. Nanomedicine 2006;2(3):158–68.
[22] Liu X, Ren X, Deng X, Huo Y, Xie J, Huang H, et al. A protein interaction network for the analysis of the neuronal differentiation of neural stem cells in response to titanium dioxide nanoparticles. Biomaterials 2010;31(11):3063–70.
[23] Jeon YM, Son BS, Lee MY. Proteomic identification of the differentially expressed proteins in human lung epithelial cells by airborne particulate matter. J Appl Toxicol 2011;31(1):45–52.
[24] Lok CN, Ho CM, Chen R, He QY, Yu WY, Sun H, et al. Proteomic analysis of the mode of antibacterial action of silver nanoparticles. J Proteome Res 2006;5(4):916–24.
[25] Tedesco S, Doyle H, Blasco J, Redmond G, Sheehan D. Exposure of the blue mussel, Mytilus edulis, to gold nanoparticles and the pro-oxidant menadione. Comp Biochem Physiol C Toxicol Pharmacol 2010;151(2):167–74.
[26] Iuso A, Scacco S, Piccoli C, Bellomo F, Petruzzella V, Trentadue R, et al. Dysfunctions of cellular oxidative metabolism in patients with mutations in the NDUFS1 and NDUFS4 genes of complex I. J Biol Chem 2006;281(15):10374–80.
[27] Grillo C, D'Ambrosio C, Scaloni A, Maceroni M, Merluzzi S, Turano C, et al. Cooperative activity of Ref-1/APE and ERp57 in reductive activation of transcription factors. Free Radic Biol Med 2006;41(7):1113–23.
[28] Jin S, Inoue S, Weaver DT. Functions of the DNA dependent protein kinase. Cancer Surv 1997;29:221–61.
[29] Krynetski EY, Krynetskaia NF, Bianchi ME, Evans WE. A nuclear protein complex containing high mobility group proteins B1 and B2, heat shock cognate protein 70, ERp60, and glyceraldehyde-3-phosphate dehydrogenase is involved in the cytotoxic response to DNA modified by incorporation of anticancer nucleoside analogues. Cancer Res 2003;63(1):100–6.
[30] Daiyasu H, Watanabe K, Toh H. Recruitment of thioredoxin-like domains into prostaglandin synthases. Biochem Biophys Res Commun 2008;369(2):281–6.
[31] Huang M, Rech JE, Northington SJ, Flicker PF, Mayeda A, Krainer AR, et al. The C-protein tetramer binds 230 to 240 nucleotides of pre-mRNA and nucleates the assembly of 40S heterogeneous nuclear ribonucleoprotein particles. Mol Cell Biol 1994;14(1):518–33.
[32] Hossain MN, Fuji M, Miki K, Endoh M, Ayusawa D. Downregulation of hnRNP C1/C2 by siRNA sensitizes HeLa cells to various stresses. Mol Cell Biochem 2007;296(1–2):151–7.
[33] Lee SY, Park JH, Kim S, Park EJ, Yun Y, Kwon J. A proteomics approach for the identification of nucleophosmin and heterogeneous nuclear ribonucleoprotein C1/C2 as chromatin-binding proteins in response to DNA double-strand breaks. Biochem J 2005;388(1):7–15.

[34] Haley B, Paunesku T, Protic M, Woloschak GE. Response of heterogeneous ribonuclear proteins (hnRNP) to ionising radiation and their involvement in DNA damage repair. Int J Radiat Biol 2009;85(8):643–55.
[35] Chappell C, Hanakahi LA, Karimi-Busheri F, Weinfeld M, West SC. Involvement of human polynucleotide kinase in double-strand break repair by non-homologous end joining. EMBO J 2002;21(11):2827–32.
[36] Jilani A, Ramotar D, Slack C, Ong C, Yang XM, Scherer SW, et al. Molecular cloning of the human gene, PNKP, encoding a polynucleotide kinase 3'-phosphatase and evidence for its role in repair of DNA strand breaks caused by oxidative damage. J Biol Chem 1999;274(34): 24176–86.
[37] Perreau J, Lilienbaum A, Vasseur M, Paulin D. Nucleotide sequence of the human vimentin gene and regulation of its transcription in tissues and cultured cells. Gene 1988;62(1):7–16.
[38] Way G, Morrice N, Smythe C, O'Sullivan AJ. Purification and identification of secernin, a novel cytosolic protein that regulates exocytosis in mast cells. Mol Biol Cell 2002;13(9):3344–54.
[39] Miyoshi N, Ishii H, Mimori K, Sekimoto M, Doki Y, Mori M. SCRN1 is a novel marker for prognosis in colorectal cancer. J Surg Oncol 2010; 101(2):156–9.
[40] Yarm FR. Plk phosphorylation regulates the microtubule-stabilizing protein TCTP. Mol Cell Biol 2002;22(17):6209–21.
[41] Price N, Proud C. The guanine nucleotide-exchange factor, eIF-2B. Biochimie 1994;76(8):748–60.
[42] Park SG, Kim HJ, Min YH, Choi EC, Shin YK, Park BJ, et al. Human lysyl-tRNA synthetase is secreted to trigger proinflammatory response. Proc Natl Acad Sci U S A 2005;102(18):6356–61.
[43] Kawamata H, Magrane J, Kunst C, King MP, Manfredi G. Lysyl-tRNA synthetase is a target for mutant SOD1 toxicity in mitochondria. J Biol Chem 2008;283(42): 28321–8.
[44] Castet A, Boulahtouf A, Versini G, Bonnet S, Augereau P, Vignon F, et al. Multiple domains of the receptor-interacting protein 140 contribute to transcription inhibition. Nucleic Acids Res 2004;32(6):1957–66.
[45] Chinnadurai G. CtBP, an unconventional transcriptional corepressor in development and oncogenesis. Mol Cell 2002;9(2):213–24.
[46] Beyenbach KW, Wieczorek H. The V-type H+ ATPase: molecular structure and function, physiological roles and regulation. J Exp Biol 2006;209(4):577–89.
[47] Pearce MM, Wang Y, Kelley GG, Wojcikiewicz RJ. SPFH2 mediates the endoplasmic reticulum-associated degradation of inositol 1,4,5-trisphosphate receptors and other substrates in mammalian cells. J Biol Chem 2007;282(28):20104–15.
[48] Kolwijck E, Zusterzeel PL, Roelofs HM, Hendriks JC, Peters WH, Massuger LF. GSTP1-1 in ovarian cyst fluid and disease outcome of patients with ovarian cancer. Cancer Epidemiol Biomarkers Prev 2009;18(8):2176–81.
[49] Fu P, Chen J, Tian Y, Watkins T, Cui X, Zhao B. Anti-tumor effect of hematopoietic cells carrying the gene of ribonuclease inhibitor. Cancer Gene Ther 2005;12(3):268–75.
[50] Zochbauer-Muller S, Fong KM, Geradts J, Xu X, Seidl S, End-Pfutzenreuter A, et al. Expression of the candidate tumor suppressor gene hSRBC is frequently lost in primary lung cancers with and without DNA methylation. Oncogene 2005;24(41):6249–55.
[51] Li L, Tao Q, Jin H, van Hasselt A, Poon FF, Wang X, et al. The tumor suppressor UCHL1 forms a complex with p53/MDM2/ARF to promote p53 signaling and is frequently silenced in nasopharyngeal carcinoma. Clin Cancer Res 2010;16(11): 2949–58.